Flying *Drosophila* maintain arbitrary but stable headings relative to the angle of polarized light

Timothy L. Warren[1,2,3], Peter T. Weir[1,4], Michael H. Dickinson[1,5]

Affiliations:

[1]Division of Biology and Biological Engineering, California Institute of Technology, Pasadena, California 91125

[2]Institute of Neuroscience, University of Oregon, Eugene, Oregon 97401

[3]Department of Botany and Plant Pathology, Oregon State University, Corvallis, Oregon 97331

[4]Data Science, Yelp, San Francisco, CA, 94111

[5]Corresponding Author

Key Words: navigation, polarized light, dispersal, sun compass, central complex, insects

SUMMARY STATEMENT

Relative to celestial cues, fruit flies select unpredictable flight headings and maintain them with gradually increasing fidelity. This may be a general dispersal strategy for animals with no target destination.

ABSTRACT

Animals must use external cues to maintain a straight course over long distances. In this study, we investigated how the fruit fly, *Drosophila melanogaster*, selects and maintains a flight heading relative to the axis of linearly polarized light, a visual cue produced by the atmospheric scattering of sunlight. To track flies' headings over extended periods, we used a flight simulator that coupled the angular velocity of dorsally presented polarized light to the stroke amplitude difference of the animal's wings. In the simulator, most flies actively maintained a stable heading relative to the axis of polarized light for the duration of 15 minute flights. We found that individuals selected arbitrary, unpredictable headings relative to the polarization axis, which demonstrates that *Drosophila* can perform proportional navigation using a polarized light pattern. When flies flew in two consecutive bouts separated by a 5 minute gap, the two flight headings were correlated, suggesting individuals retain a memory of their chosen heading. We found that adding a polarized light pattern to a light intensity gradient enhanced flies' orientation ability, suggesting *Drosophila* use a combination of cues to navigate. For both polarized light and intensity cues, flies' capacity to maintain a stable heading gradually increased over several minutes from the onset of flight. Our findings are consistent with a model in which each individual initially orients haphazardly but then settles on a heading which is maintained via a self-reinforcing process. This may be a general dispersal strategy for animals with no target destination.

INTRODUCTION

To travel long distances, both human and animal navigators employ a similar strategy of proportional navigation in which they maintain a constant heading relative to a stable distant landmark. External cues are critical for maintaining a constant heading, because navigation using purely idiothetic cues (i.e. dead reckoning) is subject to drift, resulting in circular paths (Souman et al., 2009). Whereas the sun itself is a convenient cue for proportional navigation, both the light intensity gradient produced by the sun and the pattern of polarized light caused by atmospheric scattering of sunlight serve as stable references for orientation (Von Frisch, 1967; Wehner, 1984). Insects possess photoreceptors in the dorsal region of their eye that are specialized for detecting the pattern of polarized skylight (Labhart, 1980; Wehner, 1984; Weir et al., 2016). This hardware is quite ancient and serves varied navigational tasks in many extant taxa including ants, locusts, dung beetles, and honey bees (Dacke et al., 2003; Mappes and Homberg, 2004; Rossel, 1993; Wehner, 1984).

The fruit fly, *Drosophila melanogaster*, is not considered a long-distance navigator in that, as far as we know, its populations do not follow regular seasonal patterns of movement. However, proportional navigation is of use not only to individuals or populations attempting to migrate back and forth from the same general locations, but also to animals attempting to maintain a constant heading while dispersing. Indeed, a sky compass for seasonal migration is likely a recent modification of a more general system for directed dispersal. Further, abilities of many insects to disperse over great distances is generally underappreciated because their small size renders them obscure (Lack, 1951). However, recent measurements using entomological radar indicate that insect populations move on remarkably large global scales (Hu et al., 2016). Mark and recapture experiments in Death Valley, California suggest that even fruit flies can travel up to 15 kilometers across an open desert in a single evening (Coyne et al., 1982), a feat that, due to energetic limitations, requires the maintenance of a relatively constant flight path. Prior experiments on tethered animals in flight simulators indicate that *Drosophila* can orient using a natural (Weir and Dickinson, 2012) and simulated (Wolf et al., 1980) pattern of polarized skylight. Thus, it is possible that the flies in the Death Valley experiments used this celestial cue to maintain a straight flight path.

The ability of animals to use a celestial compass to maintain a constant heading during dispersal raises an important question: which heading do they choose? One hypothesis consistent with prior observations is that, soon after initiating flight, flies choose an arbitrary direction, which they then maintain over time. Such behavior would be analogous to that exhibited by dung beetles, which upon building a dung ball, roll it away from the central heap in a straight line, but at an

arbitrary heading that they somehow choose at the beginning of their journey (Baird et al., 2010; El Jundi et al., 2016). Another possibility is that flies possesses an intrinsic heading preference perhaps biased along the axis of polarized light or perpendicular to it (Wernet et al., 2012; Wolf et al., 1980). Such an intrinsic preference would be more analogous to the behavior of migrating monarch butterflies, which fly day after day in roughly the same direction, until the preference shifts due to temperature cues (Mouritsen et al., 2013; Reppert et al., 2010).

Due to their small size, it is difficult to track the heading of individual flies in an outdoor release experiment. In this study, we employed an alternative approach of testing a large number of individuals in a flight simulator. We find that flies select arbitrary, unpredictable headings, resulting in a broad distribution that deviates only slightly from a uniform one. Our results provide insight into how *Drosophila* might employ the polarized light system for long distance dispersal.

MATERIALS AND METHODS

Fly Tethering

We tested 3- to 4-day-old female *D. melanogaster* from two distinct lines ('Phinney Ridge' and 'Top Banana'), derived from wild-caught flies collected in Seattle, Washington in 2012-2013. We observed no significant difference in performance between the two lines. To maintain genetic variability, each line was propagated with a large number of parents (~100 flies). Experiments were conducted April 2013 - March 2015.

We immobilized flies by tethering them under cold anesthesia to a tungsten wire, bent at 60°. One end was glued to the fly's anterior notum with a UV-cured adhesive (Bondic). The other was attached to a male D-Sub connector pin (Digikey A2160-ND), which mated to a female pin in our flight simulator (Fig. 1A). To prevent head movement, we immobilized the head relative to the body with glue between the head and thorax. Following anesthesia, flies recovered for at least 20 min prior to initiation of experiments.

Flight Arena

In our flight simulator, we coupled the angular velocity of an overhead light stimulus to the difference in wing stroke amplitude. Wing stroke amplitude was continuously estimated via a machine vision system (Kinefly ROS package; Suver et al., 2016; frame rate, 60 Hz). A digital camera (Basler-602AF), equipped with a macro lens and IR filter (Computar MLM3x-MP; Hoya IR filter)

captured wing images from a 45° mirror beneath the fly (Thorlabs H45A), with IR illumination provided by an optical fiber above the fly.

An LED spotlight beneath the fly provided illumination for the visual stimulus. Light was transmitted through a rotating polarizer (or intensity filter) and then reflected to the fly eye off an overhead spherical mirror with protected aluminum coating, reflecting >80% of UV light and >90% of blue light (Fig. 1A; Edmunds Optics 43-469). This optical path restricted the stimulus to light reflected from the mirror, thus ensuring that only light rays normal to the polarizing filter reached the eye. This avoided artefactual intensity cues, as light transmission varies with polarization angle at oblique incident angles (Wolf et al., 1980). The 45° mirror was housed on a 5 mm radius mount that prevented polarized light from reaching the fly directly from below. We used four stimulus configurations: linear polarizer, circular polarizer, intensity filter with linear polarizer, and intensity filter with circular polarizer. The linear polarizer (Bolder Optik BVO UV) functioned over a broad spectrum; however, the circular polarizer control (Hoya 52mm) only functioned at visible wavelengths. Therefore, to conduct control experiments most conveniently, we employed a blue illumination source (Smartvision SA30-470; peak λ, 470 nm). We compared these results with those from a UV light source (Smartvision SA30-365; peak λ, 365 nm), as insect eyes have high sensitivity to dorsally polarized light at UV wavelengths (Fortini and Rubin, 1991; Labhart, 1980; Wernet et al., 2012). At 470 nm, polarized light transmission efficiency in the preferred direction was 0.78 with an overall 99.7% degree of polarization. At 365 nm, transmission in the preferred direction was 0.38 with a 97.2% degree of polarization. The light intensity of polarized light reaching the eye was 3.44 mW cm^{-2} (measured at 470 nm). To create a light intensity gradient, we used a graduated neutral density filter (Tiffen 52 Grad ND 0.6), which reduced transmission by 2 logarithmic steps, similar to prior experimental measurements at a 12° sun angle (el Jundi et al., 2014). For the combined intensity and linear polarizer stimulus, the polarization axis was oriented perpendicular to the intensity gradient, as occurs naturally.

We estimated the angular range of stimulus elevation to be 42°-78° above the horizon (Fig. 1A, D). Lower elevations were limited by the outside of the spherical mirror (radius 22 mm) and higher elevations by the 45° mirror mount (radius 5 mm). We used a map of ommatidial orientation (Buchner, 1971) to estimate that 230/1398, or 16.5%, of ommatidia were oriented towards the stimulus in our apparatus. Assuming that the dorsal rim area (DRA) samples evenly over the dorsal hemisphere, at least 20% (36°/180°) of the frontal DRA was illuminated by our stimulus.

A stepper motor linked to a timing belt controlled stimulus rotation. The timing belt connected a small pulley (Stock Drive Products) on the stepper motor shaft (NEMA-17 Bipolar, 10,000 microsteps per rotation) to a large pulley fitted around the housing of the polarizing filters. There were 2.75 rotations of the small pulley for every stimulus rotation. We used a downward-facing photodiode combined with a stationary linear polarizing filter to monitor the rotating stimulus.

We used two similar gain functions to convert measured wing stroke difference to stimulus angular velocity. In 188/372 experiments with linear polarizer, we used a linear gain function, $\omega = k\theta$ (θ, right-left wing angle in degs; ω, angular velocity of rotating light stimulus in degs sec^{-1}; k, 1.11 sec^{-1}). In other experiments, we used an asymptotic nonlinear gain function, $\omega = 2\alpha/(1 + e^{-c\theta}) - \alpha$ (α, angular velocity limit of 65.5 deg s^{-1}; c, 0.174). For the linear polarizer, the mean local vector strength was slightly higher with the linear gain function (linear gain: 0.48 +/- 0.18; nonlinear gain: 0.55+/- 0.16; mean +/- s.d.). However, for the circular polarizer, the mean local vector strength was slightly higher for the nonlinear gain function (linear gain: 0.25 +/- 0.16; nonlinear gain: 0.32 +/- 0.15). We combined data obtained with the two gain functions as the rotational response was similar over observed wing stroke differences and both gain functions led to similar stabilization performance.

Experimental protocols

We kept flies in a dim room with lights off prior to each trial. To prevent flies from flying before each experiment, we provided a small paper piece which they held with their legs. Prior to closed-loop flight with the overhead stimulus (e.g. linearly polarized light), flies flew for one min in closed-loop with a vertical dark stripe on LED panels at the arena perimeter. The initial stimulus position for the trials with the overhead stimulus was set randomly relative to the fly's body axis. Flies were allowed to fly for 15 min; however, the experiment was halted and data discarded if flies stopped flying more than once.

For paired experiments, flies flew two 15 min closed-loop trials separated by a 5 min interruption. During the interruption, we treated flies in two distinct ways. In an unperturbed cohort (N=61), we left individuals in place in the flight simulator and minimized disruption, only interfering to prevent flies from flying. In a perturbed cohort (N=70), we removed flies from the simulator after the first flight, gave them a small piece of paper, and then re-inserted them into the apparatus after 5 min. In the second flight, the initial polarizer position was deliberately set to a new random

position. In a subset of individuals (Fig. 7), we flew flies for 10 min with open-loop rotation of the linear polarizer (0.33 Hz rotation) prior to the initiation of 15 min closed-loop flight. In a matched subset of flies, we rotated the polarizer with the same protocol but the illumination source was turned off so there was no visual stimulus.

Data acquisition and analysis

All experiments were implemented in Python and ROS (www.ros.org). Incoming video was collected at 60 Hz and stimulus position data at 200 Hz. We performed all subsequent data analyses using custom code in Python; figures were constructed using Python and FigureFirst (Lindsay et al., 2017). For offline analysis, the sampling rates of both data streams were resampled to 40 Hz. We computed *mean heading* over a given flight segment as the mean angle resulting from vector summation, with each angular measurement as a unit vector. For the axially symmetric polarized light stimulus, we computed a *mean axial heading* (range of 0-180 °) by doubling the measured headings, computing the mean resultant angle, and then halving the result (Batschelet, 1981). To determine an individual's fidelity to the mean heading, we calculated *vector strength*, a normalized measure of the vector length, obtained by summing unit vectors corresponding to each angular heading. We computed *local vector strength,* a measure of short-term heading stability, by convolving a 30 sec Gaussian filter with the orthogonal projections of the unit heading vectors and then computing the time-varying vector strength. We defined the *instantaneous heading* as the direction of the the time-varying resultant vector. We computed local vector strength for all stimuli using standard vector summation (i.e. where opposite vectors cancel rather than sum). For various analyses (e.g. Fig. 3C, D and Fig. 6 C, F), we computed the relative occupancy (i.e. probability of observing data) at different combinations of instantaneous mean heading and local vector strength. For these analyses, we binned local vector strength in 20 equal bins ranging from 0 to 1, and the instantaneous mean heading in 72 bins ranging from 0 to 360 °. For analyses of local vector strength over time, we fit experimental data with an exponential function approaching asymptote: $V(t) = V_0 + V_{offset} * (1 - e^{-t/\tau})$ in which V(t) is local vector strength; V_0 is initial vector strength; V_{offset} is asymptote; t is time, and τ is a time constant.

We used the Hodges-Ajne test, implemented in the pycircstat Python toolbox (https://github.com/circstat/pycircstat), to test the uniformity of the mean heading distribution in polarized light experiments (Fig. 3A). For statistical analyses of significant differences between groups, we used Fisher's exact test with 10,000 permutations (Fisher, 1937). To estimate confidence

intervals (e.g. Fig. 3D), we resampled from the original data set with replacement 10,000 times. The data associated with this paper are available in a Dyrad repository (doi:10.5061/dryad.gj706).

Abbreviations

CV (Coefficient of Variation), DRA (Dorsal Rim Area), IR (infrared), UV (ultraviolet), λ (wavelength)

RESULTS

To study orientation using a controlled visual stimulus, we constructed a simulator in which a tethered fly's wing strokes determined the angular velocity of a dorsally presented pattern of linearly polarized light (Fig. 1A, B). Light was projected through a rotating polarizing filter and reflected onto the fly via an overhead spherical mirror, ensuring an optical path that minimized unintended intensity cues from off-axis light (Wolf et al., 1980). When the left wing stroke amplitude was higher than the right, the polarizer rotated counterclockwise (and vice versa), providing the fly with closed-loop visual feedback. By reflecting light from above, we targeted the dorsal rim area (DRA), which is specialized for processing polarized light. Due to the limited angular extent of illumination in the apparatus, the polarized light stimulus reached only approximately 20% of the DRA and 16% of all ommatidia (Fig. 1A, D; Methods). Although the stimulus was spatially sparse, one purported function of the polarization system in insects is to provide orientation information when only small patches of sky are visible (Henze and Labhart, 2007; Von Frisch, 1967).

An example of a fly orienting to blue polarized light (470 nm peak) is shown in Fig. 1E. In this example, the fly held the polarized light axis over a 15 min flight at two distinct orientations to its body axis, 50° and 230° – a 180° offset that matches the periodicity of the polarized light pattern. As a control, we replaced the linear polarizing filter with a circular polarizer, which eliminates directional cues from polarized light itself but preserves other possible unintended orientation cues linked to stimulus rotation (e.g. light intensity fluctuations and motor vibrations). An example flight with a rotating circular polarizer is shown in Fig. 1F. In this case, there is no apparent stimulus stabilization; the polarizer drifts haphazardly over a broad range of headings.

Across a large number of flights in distinct individuals, we found that flies' capacity to stabilize rotation of the linear polarizer gradually increased over 15 min. We evaluated this time dependence using local vector strength, a metric computed by convolving the heading with a 30 sec Gaussian filter (top panels, Fig. 1E, F). Overall, there was a broad distribution of local vector

strength values in the linear polarizer data, with two small maxima at the ends of the data range. The distributions were nearly identical for UV (365 nm) and blue light (470 nm) (Fig. 2A, mean of 0.52 for both wavelengths). In contrast, the distribution from trials using a circular polarizer was sharply skewed towards 0 (Fig. 2A, mean 0.31, 470 nm). Over the 15-min flight, we observed that the average local vector strength gradually increased in a manner well-fit by an exponential function (blue light: increase from 0.40 to 0.58, τ = 5.4 minutes; UV light: increase from 0.30 to 0.61, τ = 4.6 minutes). As expected, we did not observe any such increase in local vector strength with the circular polarizer (Fig. 2B). The divergent responses to the linear and circular polarizer confirm that flies were using linearly polarized light to stabilize stimulus rotation in our apparatus. The increasing vector strength suggests that flies gradually become better at stabilizing the stimulus.

Flies maintained stable headings over the 15 min flight, a tendency apparent in an aligned occupancy histogram in which angular position reflects divergence from the mean heading (0°) and radial coordinates correspond with local vector strength (Fig. 2C). In this histogram, occupancy was tightly concentrated around the 0°/180° axis; 40° transects aligned with the mean initial heading (-20-20°, 160-200°) showed a marked skew toward higher local vector strengths compared to perpendicular transects (70-110°, 250-290°; Fig. 2C, right panel). In contrast, in controls using a circular polarizer, there was no equivalent accumulation at high local vector strengths (Fig. 2D). As a distinct measure of within-flight stability, we compared the mean heading across the two 7.5 min halves of each flight bout (Fig. 2F, G). Although there was significant variability, the data tended to cluster around the unity lines that correspond to equal headings in the two flight segments. Indeed, the observed absolute mean heading difference, 34.7°, was outside a null distribution of means obtained by repeated random shuffling of the observed headings (Fig. 2G). The mean heading difference was nearly identical (35.1°) in the 320/372 experiments in which the mean local vector strength in each 7.5 min flight segment was above a 95th percentile criterion set from the circular polarizer distribution. Taken together, these analyses suggest that flies maintain a stable heading relative to the polarization axis over a 15 min flight.

Whereas flies tended to stabilize the polarizer at a consistent heading (Fig. 2C, F, G), there was considerable inter-individual variability in the degree of stimulus stabilization. This variability is apparent in a cumulative histogram of overall axial vector strength, computed using headings from the entire flight (Fig. 2E). The coefficients of variation (CV) were 0.80 and 0.75 for UV and blue light respectively; the mean axial vector strength was 0.11 for both light sources. As expected, the

trials using a circular polarizer had low vector strength values, with little inter-individual variability (Fig. 2E, mean vector strength = .036; CV = 0.62).

Our large data set enabled us to test the hypothesis that flies preferentially align their body parallel or perpendicular to the polarization axis (Wernet et al., 2012; Wolf et al., 1980). We observed a broad distribution of mean headings (Fig. 3A). Indeed, the 10 flights with the highest vector strengths included headings over the entire range (26, 29, 39, 50, 101, 105, 116, 134, 148, and 152°). Though broad, the mean heading distribution was nonuniform ($p<.0001$; Hodges-Ajne test). To evaluate heading preference systematically, using all 93 hrs of available flight data, we computed an unaligned occupancy diagram, which binned data according to instantaneous heading and local vector strength (Fig. 3B). We observed no lateral bias in alignment (0-90° and 180-270°, 49.9% occupancy; 90-180° and 270-360°, 50.1% occupancy). We therefore combined headings from the right and left sides into a single 90° interval, ranging from headings where the principal body axis was parallel (0°) to perpendicular (90°) to the polarization axis (Fig. 3C,D; c.f. Wolf et al., 1980). The 95% confidence interval for the heading distribution, obtained via resampling, overlapped the predictions of a uniform distribution, although we did observe a small upward slope with higher probability for perpendicular than parallel headings (Fig. 3D; slope of best-fit line had a 1.1×10^{-4} change in probability per each degree of heading). The 95% confidence interval for the slope, obtained by resampling, ranged from -7.9×10^{-5} to 3.5×10^{-4}, thus encompassing zero slope (i.e. the uniform distribution). Taken together, these analyses suggest flies can maintain arbitrary headings relative to the polarization axis albeit with a slight bias towards perpendicular headings.

Neither the initial polarizer position nor the time of day could explain the observed heading variability. Time of day could influence heading if individuals had a strong preference to travel in a particular compass direction. This is because flies would need to compensate for the sun's apparent rotation (15° CCW hr^{-1} in the northern hemisphere) to maintain a straight course. However, contrary to this hypothesis, we observed no relationship between time of day and mean axial heading (Fig. 4A). An additional analysis considering periods of high local vector strength in four successive time bins revealed no consistent change in mean heading (Fig. 4B, C).

Our hypothesis that initial polarizer position, which was set randomly, could influence flight heading was motivated by the idea that individuals might maintain a straight-line trajectory upon initial cue exposure. In practice, however, small differences in wing stroke amplitude caused the polarizer to rotate soon after flight onset, making this unlikely (e.g. flights in Fig. 1E, F). Indeed, there was no relationship between starting polarizer position and mean axial heading (Fig. 4D); nor

was there a relationship between start position and the distribution of instantaneous headings (Fig. 4E, F). This lack of influence of putative extrinsic factors on heading preference suggests that variability is an intrinsic feature of flies' orientation to polarized light cues.

The heading variability we observe raises the question of whether an individual's heading choice remains constant or is reset across multiple flights. To address this question, we monitored flies' orientation preference over two 15 min flights, separated by a rest interval of 5 min. We hypothesized that perturbation during the rest interval might diminish the flies' retention of their initial heading preferences. Therefore, we treated flies in two ways during the rest interval. In an unperturbed cohort (N=61), we left the flies in place in the flight simulator and minimized disruption, only interfering to stop and later initiate flight. In a perturbed cohort (N=70), we removed flies from the simulator after the first flight, gave them a paper piece which they typically actively manipulated with their legs, and then re-inserted them into the apparatus after 5 min. Figures 5A, B show data from an unperturbed and perturbed experiment. In both examples, the heading difference between flights was small (16.1° unperturbed, 6.2° perturbed). Overall, the absolute mean heading difference for the unperturbed flies was 35.0°, significantly smaller than expected by chance (Fig. 5C, D; p=0.001, random shuffling across individuals), and nearly identical to the difference of 34.7° observed across the two 7.5 min halves of a 15 min flight (Fig. 2G). In the perturbed condition, the heading difference of 40.9° was larger but still below chance levels (p=0.035). These data demonstrate that flies retain some memory of their initial heading after a 5 min interruption.

The relatively weak heading retention observed in the perturbed cohort suggests that the flight interruption could induce a partial resetting of orientation preference. This would be reminiscent of dung beetles, who reset their travel heading each time they make a new ball (Baird et al., 2010). An alternative possibility, however, is that the flight interruption itself has no effect, and that instead the observed heading difference is consistent with the drift expected if the fly had flown continuously during the rest interval. We distinguished these possibilities by comparing the heading difference across the rest interval with that observed across an equal time gap within flight (Fig. 5G). We found that the heading change was larger over the flight interruption than within flights (Fig. 5H, I). Furthermore, the magnitude of the difference was higher in the perturbed cohort (perturbed: mean within-flight difference, 40.2°; between-flight difference, 48.4°; p=0.015; unperturbed: mean between-flight diff., 36.8°; within-flight diff., 42.2°; p=0.10 for sig. difference). These data suggest

that interrupting flight introduces heading variability that is greater than expected from the drift that occurs during flight.

Previously, we noted that local vector strength increases gradually at the start of a flight bout (Fig. 2B). Does such an increase occur during a subsequent flight? We found that changes in local vector strength during the first and second flights of the perturbed cohort were quite similar (Fig. 5J, K, $\tau = 4.2$, first; $\tau = 5.4$, second flight). In the unperturbed cohort, however, the increase in vector strength during the second flight was roughly 10 times faster (Fig. 5J, K, $\tau = 3.4$, first; $\tau = 0.3$, second flight). These data suggest that there may be a link between the process of selecting an initial heading and the gradual increase in local vector strength. According to this idea, individuals begin to fly without a heading preference (i.e. in the first flight, or in the second flight following a perturbation), and initially orient haphazardly, but as they settle on a particular heading, they begin to stabilize their course, resulting in an increased local vector strength. Consistent with this notion, flies in the perturbed cohort exhibited a vector strength increase in the second flight (Fig. 5K) and reset their heading between flights. (Fig. 5I). In contrast, in the unperturbed cohort, there was no increase in local vector strength in the second flight and the heading choice was largely inherited from the first flight.

The experiments described so far have examined flies' orientation to an isolated polarization cue. With a real sky, however, animals typically have access to multiple celestial cues, including the sun or moon, as well as intensity and chromatic gradients (el Jundi et al., 2014). Indeed, the 180° ambiguity of polarized light makes it most useful in combination with other cues. Whereas flies could potentially disambiguate the polarization pattern with a single celestial object (e.g. the sun or moon), other cues such as the intensity gradient are visible over a wider region of sky. We tested flies' capacity to integrate intensity information with the polarized light pattern by evaluating whether a combined intensity and polarizer stimulus enhanced orientation responses relative to an intensity cue on its own. We found that an intensity cue, with or without the inclusion of a linear polarizer, induced flies to maintain a single, unipolar heading. This is apparent in two example flights (Fig. 6A, B), and in aligned, 2-D occupancy diagrams (Fig. 6C); unlike in the trials with just a linear polarizer (Fig. 2C, D), there is a single peak at 0°.

We found that flies' orientation performance was superior with the combined intensity, linear polarizer stimulus than with the isolated intensity cue. Flies' enhanced fidelity to their chosen mean heading is apparent in the aligned occupancy diagrams in Fig. 6C. Indeed, there was 24.4 % more occupancy in the 40° transect centered around the mean (Fig. 6C, -20 to 20°, local vector

strength> 0.8; intensity+polarizer fraction, 0.056, intensity fraction, .045). Furthermore, overall vector strengths were significantly higher for the combined stimulus relative to the sole intensity stimulus (Fig. 6D; intensity+polarizer mean, 0.17, intensity mean, 0.14; difference at 95.2 percentile of null distribution obtained by resampling). In addition to boosting flies' vector strength, we found that including the linear polarizer narrowed the distribution of mean headings. In both cases, flies exhibited a clear preference for the dark side of the stimulus field. This is apparent when flight headings are plotted as a function of mean vector strength (Fig. 6E) and also in unaligned 2-dimensional occupancy diagrams (Fig. 6F). With the combined intensity, linear polarizer cue, the data was more tightly distributed around 180° (Fig. 6G). Taken together, our data suggest that *Drosophila* can integrate intensity and polarized light information, as the polarized light cue both enhances local vector strength within a flight and sharpens the overall heading distribution.

With both the isolated intensity cue and the combined intensity, linear polarizer stimulus, flies' local vector strength gradually increased with dynamics that closely matched those observed with the linear polarizer alone (Fig. 7A; τ = 5.7 min, intensity and linear polarizer; τ = 3.4 min, intensity alone; τ = 5.2 min, linear polarizer alone). Whereas one possibility is that this increase in local vector strength is due to individuals gradually deciding on a heading, a non-mutually exclusive explanation is sensorimotor facilitation. For example, flies' perceptual capacity could gradually improve with continued stimulus exposure due to contrast or light adaptation (Baccus and Meister, 2002; Laughlin and Hardie, 1978). To evaluate this hypothesis, we tested whether a 10 min sensory exposure to the linear polarizer could induce an increase in local vector strength equivalent to that observed in closed-loop flight. Our experimental protocol is illustrated in Fig. 7B. For the first 10 min, the fly flew with the polarized light pattern rotating at 120 $^{\circ}$ s^{-1} in open-loop, followed by a 15 min bout of closed-loop flight. We found that individuals with early stimulus exposure exhibited a subsequent local vector strength increase that closely matched that of flies with no prior sensory experience (Fig. 7C). Initial local vector strength values were closely matched (0.36 with light-exposed vs 0.39 in controls) and increased with similar temporal dynamics (τ = 4.67 for light-exposed vs 5.23 for controls). However, individuals with initial light exposure reached a lower asymptotic level (0.49 for light-exposed vs 0.59 for controls), a result for which we have no obvious explanation. Nevertheless, these data suggest that early sensory exposure to polarized light is not sufficient to induce the vector strength increase observed in closed-loop flight. In an additional cohort of flies, we removed the visual stimulus during the 10 min. period (i.e. flies flew in the dark).

In these individuals, local vector strength began at a lower level than the other two groups but increased to the same level over 15 min. This finding suggests that previous sensory experience may influence closed-loop flight performance. One possible explanation for the light-on/light-off difference is that flying in the dark is deleterious to subsequent performance, resulting in low initial vector strength. Taken together, these experiments argue against the possibility that the vector strength increase is primarily due to sensory adaptation.

DISCUSSION

In this study, we examined how *Drosophila* choose and maintain flight headings relative to an overhead pattern of polarized light as well as to an intensity gradient. Consistent with previous reports (Weir and Dickinson, 2012; Wolf et al., 1980), we found that flies can maintain a stable heading relative to the angle of polarized light (Fig. 2 C, F). Across a large population, the heading distribution was remarkably broad, with only a slight deviation from a uniform distribution, indicating that flies have a capacity to maintain arbitrary headings relative to the polarization axis (Fig. 3D). Individual flies stably maintained a heading during a 15 min flight and retained some orientation preference in a subsequent flight following a 5 min rest interval (Fig. 5 D, F); however, this interruption of flight introduced a larger heading change than observed across a similar time period during continuous flight (Fig. 5H, I). The overall variability in heading preference could not be explained by external factors such as initial start angle or time of day (Fig. 4). We found that polarized light enhanced flies' capacity to orient to an intensity gradient (Fig. 6E, I). For both polarization cues and intensity cues, flies gradually increased the extent to which they stabilized the stimulus over the 15 min flight (Fig. 7A).

Whereas certain iconic navigators such as locusts, monarch butterflies, desert ants, and honeybees have a well-documented ability to orient with sky cues (Brower, 1996; Mappes and Homberg, 2004; Wehner, 1984; Wehner, 2003), our findings support the idea that a latent capacity for celestial navigation is shared widely across insects (Dickinson, 2014). Prior evidence that *Drosophila* can navigate using sky cues includes both release-and-recapture experiments (Coyne et al., 1982; Jones et al., 1981), as well as direct manipulations of the polarized light pattern (Weir and Dickinson, 2012; Wernet et al., 2012; Wolf et al., 1980). Earlier studies showed that tethered flies can maintain a stable heading using an artificial polarized light pattern (Wolf et al., 1980) and that flies require polarized light to maintain a straight course under the natural sky when the sun is not visible (Weir and Dickinson, 2012). A key finding of our study is that individuals can maintain arbitrary

headings relative to the polarized light angle. The broad heading distribution we observed, which was slightly biased to perpendicular headings, contrasts with conclusions of a pioneering earlier report that individuals strongly bias their principal body axis parallel or perpendicular to the polarized light angle (Wolf et al., 1980). This discrepancy likely reflects the much larger size of our data set, 372 individuals with 15 min flights, compared to 36 individuals (21 of whom were visual mutants).

Our finding that *Drosophila* maintain arbitrary headings to the angle of polarized light indicates that they can perform proportional navigation, a sensory-motor strategy used for many behaviors (Murtaugh and Criel, 1966). If an agent maintains a constant bearing to an object at infinity, it will travel in a straight line. This tactic is used by humans (Souman et al., 2009), as well as by monarch butterflies and migrating birds (Mouritsen et al., 2013; Wiltschko and Wiltschko, 2003). If the object is nearby, however, the same algorithm results in a spiraling interception course, which explains why moths steer towards bright lights at night (Muirhead-Thompson, 2012). A classic proportional navigation tactic is the constant bearing/decreasing range strategy used by flying bats, dragonflies, and baseball outfielders to intercept targets (Chapman, 1968; Ghose et al., 2006; Olberg et al., 2000). In a complementary fashion, competent ship captains avoid collisions by vigilantly watching for constant bearing to other vessels, whereas frigate captains chased down potential prizes using the same principle (O'brian, 1990). Orienting according to the pattern of polarized light in the sky is equivalent to executing proportional navigation to a single celestial object at infinity. It is therefore a particularly useful means of maintaining a fixed course.

The variable flight behavior we observed is qualitatively distinct from the stereotyped orienting reflexes exhibited by flying and walking *Drosophila.* In flight simulators, flies typically position salient visual or olfactory cues either directly in front or behind them. For instance, flies orient a dark vertical stripe, or attractive odors such as vinegar, in front (Duistermars et al., 2009; Götz, 1987). Other visual stimuli and aversive odors evoke anti-fixation responses, in which flies position the stimulus behind (Maimon et al., 2008; Wasserman et al., 2012). The flight behavior we observed therefore is consistent with navigation using faraway objects, which are not attractive or aversive in themselves but instead a means to maintain a straight course.

The variable headings we observed are reminiscent of dispersal patterns observed in other insects that, like *Drosophila*, have no particular target destination. A particularly well-documented example of random dispersal is ball-rolling by dung beetles, which choose random headings relative to celestial cues when rolling balls from a central starting position. Individual beetles do not exhibit

any innate heading preference; instead, they reset their heading choice randomly each time they make their dung ball (Baird et al., 2010). Our results suggest that a similar resetting process might occur between flights in *Drosophila*, as we observed a larger heading difference between flights than over the same time interval within a flight (Fig. 5H, I). However, our findings do not rule out the possibility that flies have an innate heading preference, as we observed significant retention of heading preference following a 5 min gap (Fig. 5C, F). It seems likely that the magnitude of heading retention would diminish over longer time intervals given the effects of perturbation during the gap between flights (Fig. 5F, H). Our results suggest that there is intrinsic variability in flies' heading choices that cannot be easily explained by external factors such as time of day or initial stimulus conditions (Fig. 4). Whether the variability occurs primarily across a population or within an individual, our findings contribute to an emerging notion that precisely controlled, routine behaviors can remain highly variable (Gordus et al., 2015; Kain et al., 2012; Kao et al., 2005).

Despite the apparent contrast between the random, variable headings of dung beetles and fruit flies and the more predictable preferences of monarch butterflies and desert ants, the underlying mechanisms of navigation may be highly similar. Recent work has suggested monarchs rely primarily on proportional rather than true navigation to travel to a specific map location (Mouritsen et al., 2013). For monarchs to travel at a particular heading using proportional navigation, they must have a latent capacity to fly at arbitrary headings; that is, they must be able to select specific variants from the broad heading distribution adopted by fruit flies and dung beetles. An intriguing possibility, not addressed in our study, is that *Drosophila,* when motivated by environmental cues such as temperature and day length, might similarly select specific headings relative to celestial cues.

Flies' fidelity to their eventual mean heading gradually increased over a 15 min flight, even with exposure to the polarized light pattern for 10 min before closed-loop flight (Fig. 2B, Fig. 7). At first consideration, this gradual improvement contrasts with dung beetle trajectories, which are remarkably straight from initiation (Dacke et al., 2013). However, when beetles make a new ball, they choose a heading prior to ball-rolling during a preparatory ritual in which they scan the visual scene and take a virtual snapshot of available orientation cues (El Jundi et al., 2016). Flies could be doing an analogous sampling of the visual scene early in flight prior to selecting a specific, fixed heading. Indeed, one explanation for the gradual increase in heading fidelity we observed is that the flies might operate in a different behavioral context during the first few minutes of each flight bout. In the initial moments after take-off, the flies might search visually for a suitable landing site,

whereas later they choose a fixed heading to disperse over longer distances. Consistent with this view, we observed no gradual increase in local vector strength in the second of paired flights in unperturbed flies (Fig. 5K), presumably because heading preference had already coalesced (Fig. 5D). Our results raise the possibility that a similar gradual increase in heading fidelity might occur in other contexts where complete flight trajectories were not tracked due to experimental limitations, such as the Death Valley release-and-recapture experiments (Coyne et al., 1982).

We observed that flies' orientation performance was similar with blue and UV light (λ = 470 nm and 365 nm, respectively, Fig. 2B, E), consistent with the observation that removing UV light only causes a small decrement in flies' capacity to orient to polarized skylight (Weir and Dickinson, 2012). Together, these results indicate that the *Drosophila* visual system is sensitive to the polarization angle of dorsally presented light at λ>400 nm. One possibility is that this sensitivity is conferred by R1-R6 photoreceptors, previously implicated in ventral polarization responses (Wernet et al., 2012). Alternatively, the sensitivity of R7/R8 photoreceptors in the DRA could extend into the visible spectrum, beyond the UV wavelengths where they are most sensitive (Weir et al., 2016).

In addition to serving as a reference cue on its own, the polarization pattern enhanced flies' capacity to orient to an intensity gradient (Fig. 6). This finding demonstrates that flies opportunistically take advantage of available orientation cues, as occurs in other animals. For example, desert ants can navigate when their DRA is painted over and the sun is simultaneously shielded, leaving intensity and chromatic cues available (Wehner, 1997). Similarly, dung beetles can maintain a heading when one of two initial celestial orientation cues is removed (El Jundi et al., 2016). We observed a nonrandom heading distribution to the intensity gradient, as flies tended to position the dark side of the gradient in front, with or without the linear polarizer. This suggests that for *Drosophila*, the intensity cue may be hierarchically superior to polarized light, the reverse of observations in diurnal dung beetles (el Jundi et al., 2014). In diurnal beetles, when the sun itself is visible, it dominates both polarization and intensity cues (el Jundi et al., 2014) and therefore may also be hierarchically superior in *Drosophila*.

One notable feature of this orientation behavior was the high inter-individual variability in performance compared to other psychophysical tasks such as fixation of a salient visual landmark. Whereas many flies oriented to a specific heading with high fidelity, a sizable proportion of flies failed to display a robust orientation preference. This could be partly because the stimulus in our flight arena was small in angular extent compared to a natural sky (Fig. 1A) and lacked gradients in color, intensity, as well as the degree and angle of polarization. Furthermore, the 180° periodicity of

polarized light increases the difficulty of stabilization compared to a conventional visual panorama such as a vertical stripe. However, the large variability across flies cannot be explained entirely by these factors, as some flies stabilized the pattern well, whereas others exhibited a performance indistinguishable from circular polarizer controls. We used fly strains derived from >100 wild caught females and propagated with protocols designed to maintain genetic diversity. Thus, the large differences in performance that we measured might have a genetic basis. If true, this would be noteworthy as it might reflect an ecologically relevant variability in dispersal predilection of natural populations.

Pairing the celestial navigation paradigm we describe in this study with novel techniques to monitor neural activity during behavior could reveal general principles of how the nervous system performs sensory-motor transformation. Recent studies in *Drosophila* have identified neural maps in columnar neurons of the central complex that correspond topographically to an animal's heading in walking or flight (Kim et al., 2017; Seelig and Jayaraman, 2015). In quiescent locusts and dung beetles, homologs of these neurons similarly map celestial stimuli (el Jundi et al., 2015; Heinze and Homberg, 2007). Therefore, the behavioral paradigm we introduce here, in head-fixed flies, is well-suited for physiology and could enable functional studies of these putative orientation maps**.** Our study demonstrates that the underlying mechanisms of the navigation must involve generation of heading variability, maintenance of memory, and integration across multiple visual cues.

ACKNOWLEDGEMENTS

We thank Nicole Iwasaki for assistance with data collection.

COMPETING INTERESTS

No competing interests declared.

FUNDING

This work was supported by the National Science Foundation grant IBN-1352707 (to M.H.D.).

REFERENCES

Baccus, S. A. and Meister, M. (2002). Fast and slow contrast adaptation in retinal circuitry. *Neuron* **36**, 909-919.

Baird, E., Byrne, M. J., Scholtz, C. H., Warrant, E. J. and Dacke, M. (2010). Bearing selection in ball-rolling dung beetles: is it constant? *Journal of Comparative Physiology A: Neuroethology, Sensory, Neural, and Behavioral Physiology* **196**, 801-806.

Batschelet, E. (1981). Circular statistics in biology. *ACADEMIC PRESS, 111 FIFTH AVE., NEW YORK, NY 10003, 1981, 388*.

Brower, L. (1996). Monarch butterfly orientation: missing pieces of a magnificent puzzle. *Journal of experimental biology* **199**, 93-103.

Buchner, E. (1971). Dunkelanregung des stationaeren flugs der fruchtfliege Drosophila. Dipl. thesis. *Univ Tübingen*.

Chapman, S. (1968). Catching a baseball. *American Journal of Physics* **36**, 868-870.

Coyne, J. A., Boussy, I. A., Prout, T., Bryant, S. H., Jones, J. and Moore, J. A. (1982). Long-distance migration of Drosophila. *American Naturalist* **119**, 589-595.

Dacke, M., Byrne, M., Smolka, J., Warrant, E. and Baird, E. (2013). Dung beetles ignore landmarks for straight-line orientation. *Journal of Comparative Physiology A* **199**, 17-23.

Dacke, M., Nilsson, D.-E., Scholtz, C. H., Byrne, M. and Warrant, E. J. (2003). Animal behaviour: insect orientation to polarized moonlight. *Nature* **424**, 33-33.

Dickinson, M. H. (2014). Death valley, Drosophila, and the Devonian toolkit. *Annual review of entomology* **59**, 51-72.

Duistermars, B. J., Chow, D. M. and Frye, M. A. (2009). Flies require bilateral sensory input to track odor gradients in flight. *Current biology* **19**, 1301-1307.

El Jundi, B., Foster, J. J., Khaldy, L., Byrne, M. J., Dacke, M. and Baird, E. (2016). A snapshot-based mechanism for celestial orientation. *Current biology* **26**, 1456-1462.

el Jundi, B., Smolka, J., Baird, E., Byrne, M. J. and Dacke, M. (2014). Diurnal dung beetles use the intensity gradient and the polarization pattern of the sky for orientation. *Journal of experimental biology* **217**, 2422-2429.

el Jundi, B., Warrant, E. J., Byrne, M. J., Khaldy, L., Baird, E., Smolka, J. and Dacke, M. (2015). Neural coding underlying the cue preference for celestial orientation. *Proceedings of the National Academy of Sciences* **112**, 11395-11400.

Fisher, R. A. (1937). The design of experiments: Oliver And Boyd; Edinburgh; London.

Fortini, M. E. and Rubin, G. M. (1991). The optic lobe projection pattern of polarization-sensitive photoreceptor cells in Drosophila melanogaster. *Cell and tissue research* **265**, 185-191.

Ghose, K., Horiuchi, T. K., Krishnaprasad, P. and Moss, C. F. (2006). Echolocating bats use a nearly time-optimal strategy to intercept prey. *PLoS biology* **4**, e108.

Gordus, A., Pokala, N., Levy, S., Flavell, S. W. and Bargmann, C. I. (2015). Feedback from network states generates variability in a probabilistic olfactory circuit. *Cell* **161**, 215-227.

Götz, K. G. (1987). Course-control, metabolism and wing interference during ultralong tethered flight in Drosophila melanogaster. *Journal of experimental biology* **128**, 35-46.

Hardie, R. C. (2012). Polarization vision: Drosophila enters the arena. *Current biology* **22**, R12-R14.

Heinze, S. and Homberg, U. (2007). Maplike representation of celestial E-vector orientations in the brain of an insect. *Science* **315**, 995-997.

Henze, M. J. and Labhart, T. (2007). Haze, clouds and limited sky visibility: polarotactic orientation of crickets under difficult stimulus conditions. *Journal of experimental biology* **210**, 3266-3276.

Hu, G., Lim, K. S., Horvitz, N., Clark, S. J., Reynolds, D. R., Sapir, N. and Chapman, J. W. (2016). Mass seasonal bioflows of high-flying insect migrants. *Science* **354**, 1584-1587.

Jones, J., Bryant, S., Lewontin, R., Moore, J. and Prout, T. (1981). Gene flow and the geographical distribution of a molecular polymorphism in Drosophila pseudoobscura. *Genetics* **98**, 157-178.

Kain, J. S., Stokes, C. and de Bivort, B. L. (2012). Phototactic personality in fruit flies and its suppression by serotonin and white. *Proceedings of the National Academy of Sciences* **109**, 19834-19839.

Kao, M. H., Doupe, A. J. and Brainard, M. S. (2005). Contributions of an avian basal ganglia–forebrain circuit to real-time modulation of song. *Nature* **433**, 638-643.

Kim, S. S., Rouault, H., Druckmann, S. and Jayaraman, V. (2017). Ring attractor dynamics in the Drosophila central brain. *Science* **356**, 849-853.

Labhart, T. (1980). Specialized photoreceptors at the dorsal rim of the honeybee's compound eye: polarizational and angular sensitivity. *Journal of Comparative Physiology A: Neuroethology, Sensory, Neural, and Behavioral Physiology* **141**, 19-30.

Lack, E. (1951). Migration of insects and birds through a Pyrenean pass. *The Journal of Animal Ecology*, 63-67.

Laughlin, S. B. and Hardie, R. C. (1978). Common strategies for light adaptation in the peripheral visual systems of fly and dragonfly. *Journal of Comparative Physiology A: Neuroethology, Sensory, Neural, and Behavioral Physiology* **128**, 319-340.

Lindsay, T., Weir, P. T. and van Breugel, F. (2017). FigureFirst: A Layout-first Approach for Scientific Figures.

Maimon, G., Straw, A. D. and Dickinson, M. H. (2008). A simple vision-based algorithm for decision making in flying Drosophila. *Current biology* **18**, 464-470.

Mappes, M. and Homberg, U. (2004). Behavioral analysis of polarization vision in tethered flying locusts. *Journal of Comparative Physiology A* **190**, 61-68.

Mouritsen, H., Derbyshire, R., Stalleicken, J., Mouritsen, O. Ø., Frost, B. J. and Norris, D. R. (2013). An experimental displacement and over 50 years of tag-recoveries show that monarch butterflies are not true navigators. *Proceedings of the National Academy of Sciences* **110**, 7348-7353.

Muirhead-Thompson, R. (2012). Trap responses of flying insects: the influence of trap design on capture efficiency: Academic Press.

Murtaugh, S. A. and Criel, H. E. (1966). Fundamentals of proportional navigation. *IEEE spectrum* **3**, 75-85.

O'brian, P. (1990). Master and Commander (Vol. Book 1): WW Norton & Company.

Olberg, R., Worthington, A. and Venator, K. (2000). Prey pursuit and interception in dragonflies. *Journal of Comparative Physiology A: Neuroethology, Sensory, Neural, and Behavioral Physiology* **186**, 155-162.

Reppert, S. M., Gegear, R. J. and Merlin, C. (2010). Navigational mechanisms of migrating monarch butterflies. *Trends in neurosciences* **33**, 399-406.

Rossel, S. (1993). Navigation by bees using polarized skylight. *Comparative Biochemistry and Physiology Part A: Physiology* **104**, 695-708.

Seelig, J. D. and Jayaraman, V. (2015). Neural dynamics for landmark orientation and angular path integration. *Nature* **521**, 186-191.

Souman, J. L., Frissen, I., Sreenivasa, M. N. and Ernst, M. O. (2009). Walking straight into circles. *Current biology* **19**, 1538-1542.

Suver, M. P., Huda, A., Iwasaki, N., Safarik, S. and Dickinson, M. H. (2016). An array of descending visual interneurons encoding self-motion in Drosophila. *Journal of Neuroscience* **36**, 11768-11780.

Von Frisch, K. (1967). The dance language and orientation of bees.

Wasserman, S., Lu, P., Aptekar, J. W. and Frye, M. A. (2012). Flies dynamically anti-track, rather than ballistically escape, aversive odor during flight. *Journal of experimental biology* **215**, 2833-2840.

Wehner, R. (1984). Astronavigation in insects. *Annual review of entomology* **29**, 277-298.

Wehner, R. (1997). The ant's celestial compass system: spectral and polarization channels. In *Orientation and communication in arthropods*, pp. 145-185: Springer.

Wehner, R. (2003). Desert ant navigation: how miniature brains solve complex tasks. *Journal of Comparative Physiology A: Neuroethology, Sensory, Neural, and Behavioral Physiology* **189**, 579-588.

Weir, P. T. and Dickinson, M. H. (2012). Flying Drosophila orient to sky polarization. *Current biology* **22**, 21-7.

Weir, P. T., Henze, M. J., Bleul, C., Baumann-Klausener, F., Labhart, T. and Dickinson, M. H. (2016). Anatomical reconstruction and functional imaging reveal an ordered array of skylight polarization detectors in Drosophila. *Journal of Neuroscience* **36**, 5397-5404.

Wernet, M. F., Velez, M. M., Clark, D. A., Baumann-Klausener, F., Brown, J. R., Klovstad, M., Labhart, T. and Clandinin, T. R. (2012). Genetic dissection reveals two separate retinal substrates for polarization vision in Drosophila. *Current biology* **22**, 12-20.

Wiltschko, R. and Wiltschko, W. (2003). Avian navigation: from historical to modern concepts. *Animal behaviour* **65**, 257-272.

Wolf, R., Gebhardt, B., Gademann, R. and Heisenberg, M. (1980). Polarization sensitivity of course control in Drosophila melanogaster. *Journal of Comparative Physiology A: Neuroethology, Sensory, Neural, and Behavioral Physiology* **139**, 177-191.

Figures

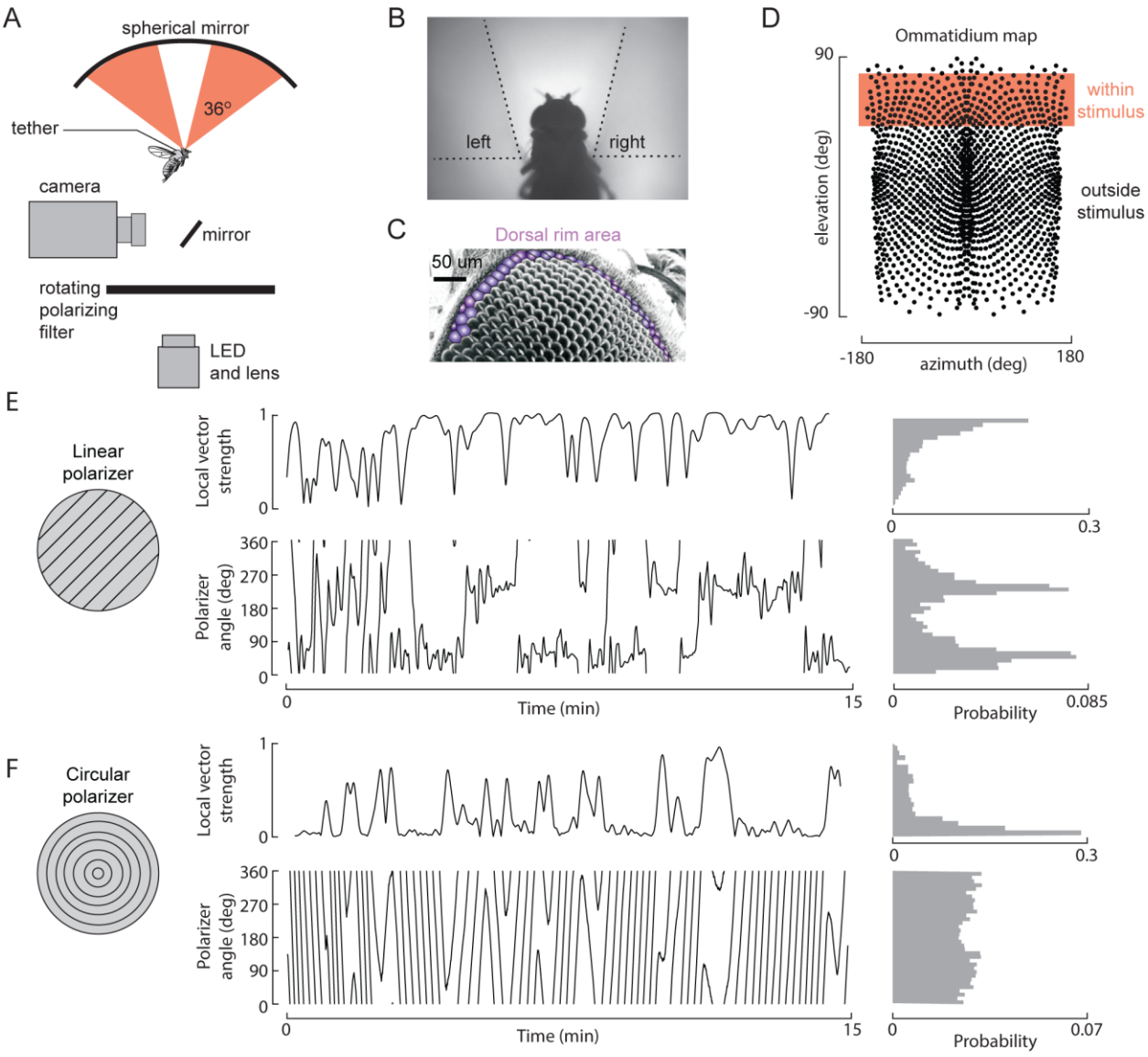

Figure 1. A closed-loop flight simulator for studying navigation to polarized light in tethered, head-fixed *Drosophila.* (A) Experimental apparatus. The difference in wing stroke amplitude, as measured by an infrared (IR) video camera, controls the angular velocity of a rotating polarizing filter. Unpolarized light (peak λ=365 or 470 nm) from LED beneath fly passes through a rotating polarizer and is reflected onto fly by an overhead spherical mirror. The incoming light

stimulus ranged from 42.1° to 78.5° of elevation (36.4° net transect). We imaged the wing strokes via a 45° mirror, which reflected light transmitted from an IR source above fly (not shown). (B) Example frame of IR video showing wing stroke envelopes. (C) Electron micrograph of *Drosophila* eye with dorsal rim area ommatidia colored purple (modified from Hardie, 2012). (D) Map of estimated stimulus size on retina (c.f. Buchner, 1971). In total, 16.5% of ommatidia (230/1398) had receptive fields covered by the stimulus. (E) Example closed-loop data using a linearly polarizing filter (λ = 470 nm). The bottom trace shows the angular position of polarizer over a 15-minute flight. At 0°/180°, the axis of polarization is aligned with fly's longitudinal body axis. The distribution of headings flown is plotted on the right; note two distinct peaks at headings of 50° and 230°. The top trace plots local vector strength, indicating degree of stimulus stabilization. A histogram of local vector strength is plotted on the right. (F) Data comparable to E, but using a circularly polarized light stimulus. Note that the fly is unable to stabilize the stimulus and local vector strength is low.

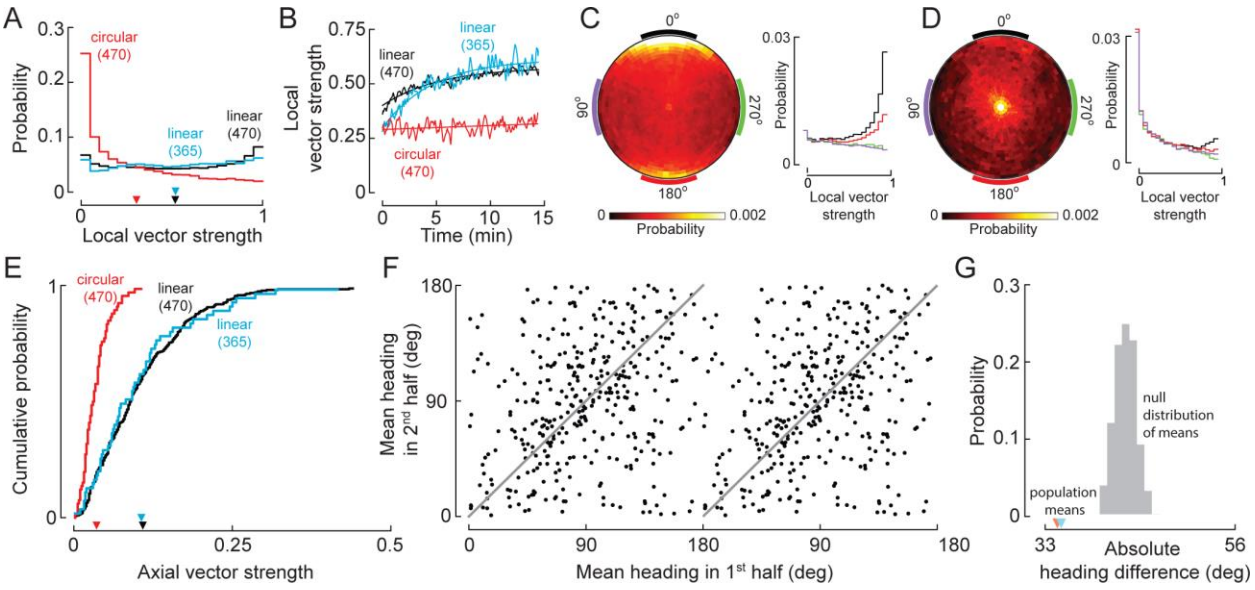

Figure 2. Tethered, flying *Drosophila* maintain stable headings relative to the angle of polarized light. (A) Distribution of local vector strength values for experiments with circularly (red, λ = 470 nm, N=66) and linearly (black, λ = 470 nm, N=317; blue, λ = 365 nm, N=55) polarized light. Means are indicated by inverted triangles. (B) Time course of mean local vector strength over 15-min flight for experimental conditions in A. Smooth lines are fits to exponential distributions. (C) Probability distribution for linearly polarized light data, aligned to mean flight heading. The circular color map is an occupancy histogram, summed across all data (N=372). An angular difference from 0° reflects divergence from an individual's mean heading. The radial distance from center of plot reflects local vector strength, varying from 0 at center to 1 at outside edge. The right panel plots the probability distributions for local vector strength within four, 40° orthogonal transects (-20°-20°, 70°-110°, 160°-200°, 250°-290°), indicated by the black, green, red, and purple arcs in the left panel. (D) Probability distribution for circularly polarized stimulus, aligned to mean flight heading; plotting conventions as in C. (E) Cumulative probability distributions of axial vector strength for circularly and linearly polarized light; colors as in A. Inverted triangles indicate distribution means. (F) Comparison of mean axial headings from 1st half (0-7.5 min) and 2nd half (7.5-15 min) of experiments using linearly polarized light (N=372). Data are repeated along the abscissa at an

interval of 180° to reflect the axial symmetry of stimulus. Grey lines correspond to identical headings. (G) Comparison between the observed heading differences between flight segments in F and shuffled controls. Inverted triangles indicate mean absolute heading difference for all data with linear polarizer (N=372, red) and for subset where mean local vector strength was above threshold set by circular polarizer distribution (n=320, blue). Histogram is null distribution of mean differences obtained by shuffling across all flights (10,000 permutations).

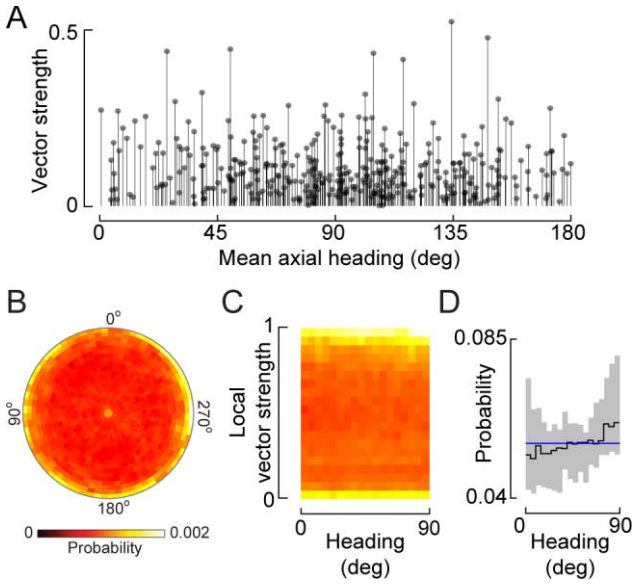

Figure 3. *Drosophila* choose arbitrary flight headings. (A) Flight headings relative to the angle of polarized light. Horizontal position of points is mean axial heading; vertical position is overall axial vector strength (N=372). The six headings with highest local vector strength values were 134, 148, 50, 26, 105, and 116°. (B) Unaligned occupancy histogram; plotting conventions as in Fig. 2C except that data were not aligned to mean heading (N=372 flies, 5,580 min of flight data). (C) Data from occupancy histogram replotted into a 90° interval ranging from parallel (0°) to perpendicular (90°) to body axis. (D) Probability distribution over 90° interval for data with local vector strength >0.8. Black line is observed distribution, corresponding to histogram in (C). Grey shaded region is 95% confidence interval, obtained by random resampling (10,000 permutations of 392 individuals). Blue horizontal line is uniform distribution.

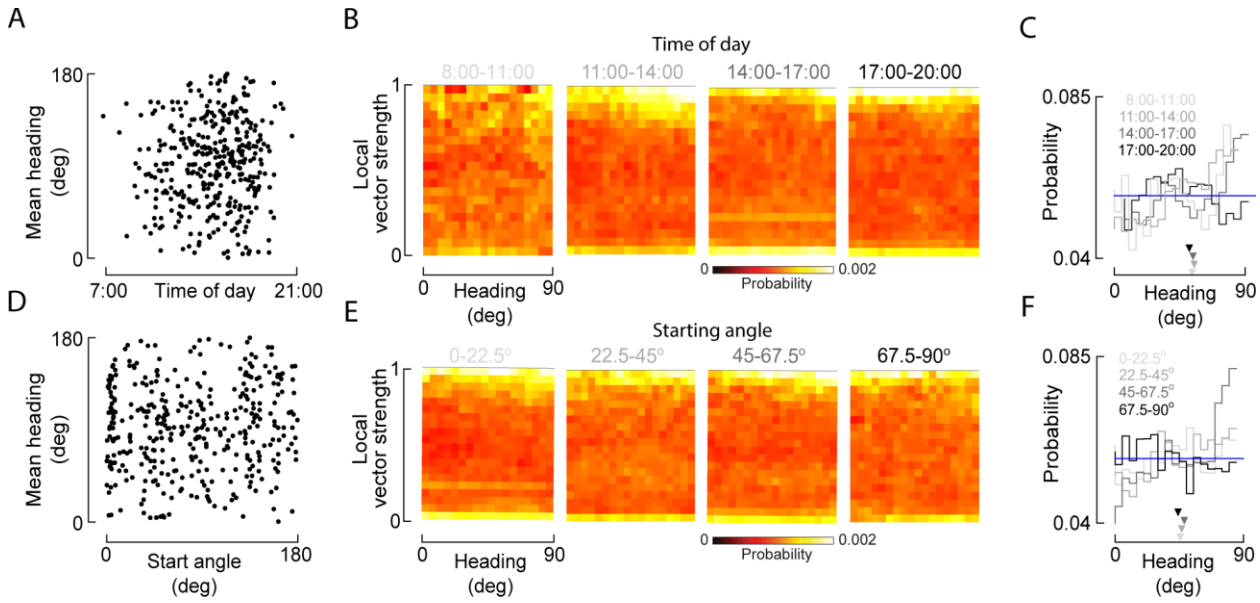

Figure 4. Time of day or polarizer position at the start of the experiment cannot explain variability in flight headings. (A) Mean axial heading as function of time at day (N=372). (B) Occupancy histograms, showing data distribution as function of axial heading and local vector strength for four consecutive time bins: 8:00-11:00 (lightest gray, N=28), 11:00-14:00 (lighter gray, N=91), 14:00-17:00 (gray, N=163), 17:00-20:00 (black, N=78). (C) Heading probabilities for data with local vector strength >0.8. Data are plotted for same time bins as in B, with same color scheme. Inverted triangles denote distribution means. (D) Mean axial heading as function of initial polarizer position at start of experiment (N=372). (E) Occupancy histograms for four non-overlapping groups of start angles: 0-22.5° (lightest gray, N=111), 22.5-45° (lighter gray, N=87), 45-67.5° (gray, N=97), and 67.5-90° (black, N=77). (F) Heading probabilities for start angle distributions shown in (E); local vector strength was >0.8.

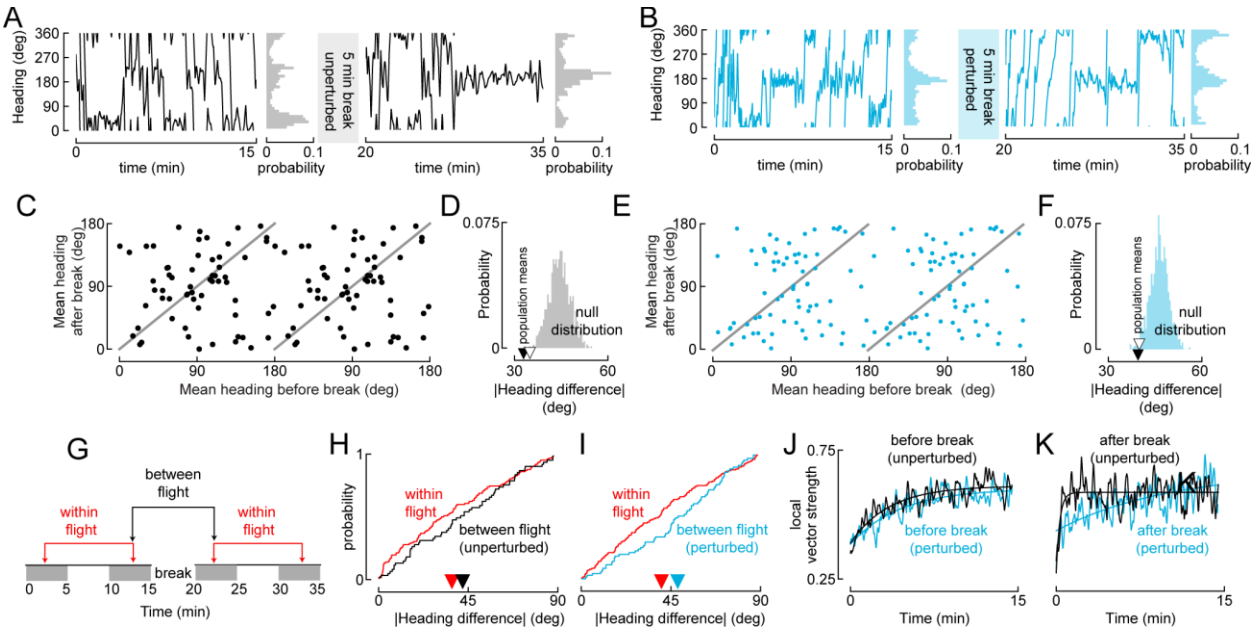

Figure 5. Flies retain a preference for their initial heading in a second flight following a 5 min break. (A) Example unperturbed experiment. Left: polarizer orientation during 1st 15-min flight (mean axial heading 25.7/205.7°). Subsequently, fly was left in apparatus for 5 min and kept from flying. Right: polarizer orientation during 2nd 15-min flight (mean heading 9.6/189.6°). (B) Example perturbed experiment. Left: polarizer orientation during 1st 15-min flight (mean axial heading 172.1/352.1°). Fly was then removed from apparatus and given paper to manipulate for 5 min. Right: polarizer orientation during 2nd 15-min flight (mean axial heading 165.9/345.9°). (C) Mean headings from 1st versus 2nd flight in unperturbed condition (N=61). (D) Absolute mean heading difference for unperturbed condition relative to shuffled distribution of means. Inverted triangles are observed means for all pairs (35.0°; N=61, white, p=.001) and for subset above threshold set by circular polarizer (33.0°; N=30, black). (E) Same convention as C for perturbed condition (N=64). (F) Same convention as D for perturbed condition (mean absolute heading difference for all flies, 40.9°; N=64, white inverted triangle, p=.035; for subset above threshold set by circular polarizer (41.0°; N=29 flies, black inverted triangle). (G) Calculation of between-flight versus within-flight differences in mean heading. For within-flight comparison, difference was calculated between 0-5 min and 10-15 min of same flight. For between-flight comparison, difference

was calculated between 10-15 min of 1st flight and 0-5 min of 2nd flight. (H) Cumulative histogram of within-flight (red) and between-flight (black) absolute mean heading difference for unperturbed flies. Inverted triangles indicate means of distributions (36.8° within-flight, 42.2° between-flight; p=0.10 for sig. difference). (I) Same conventions as H for perturbed condition (40.2° within-flight, 48.4° between-flight, p=0.015 for sig. difference). (J) Change in local vector strength during first of paired flights. Smooth lines denote best exponential fit. (K) Change in local vector strength during second of paired flights. Note the faster rise of local vector strength relative to the first flight in unperturbed trials.

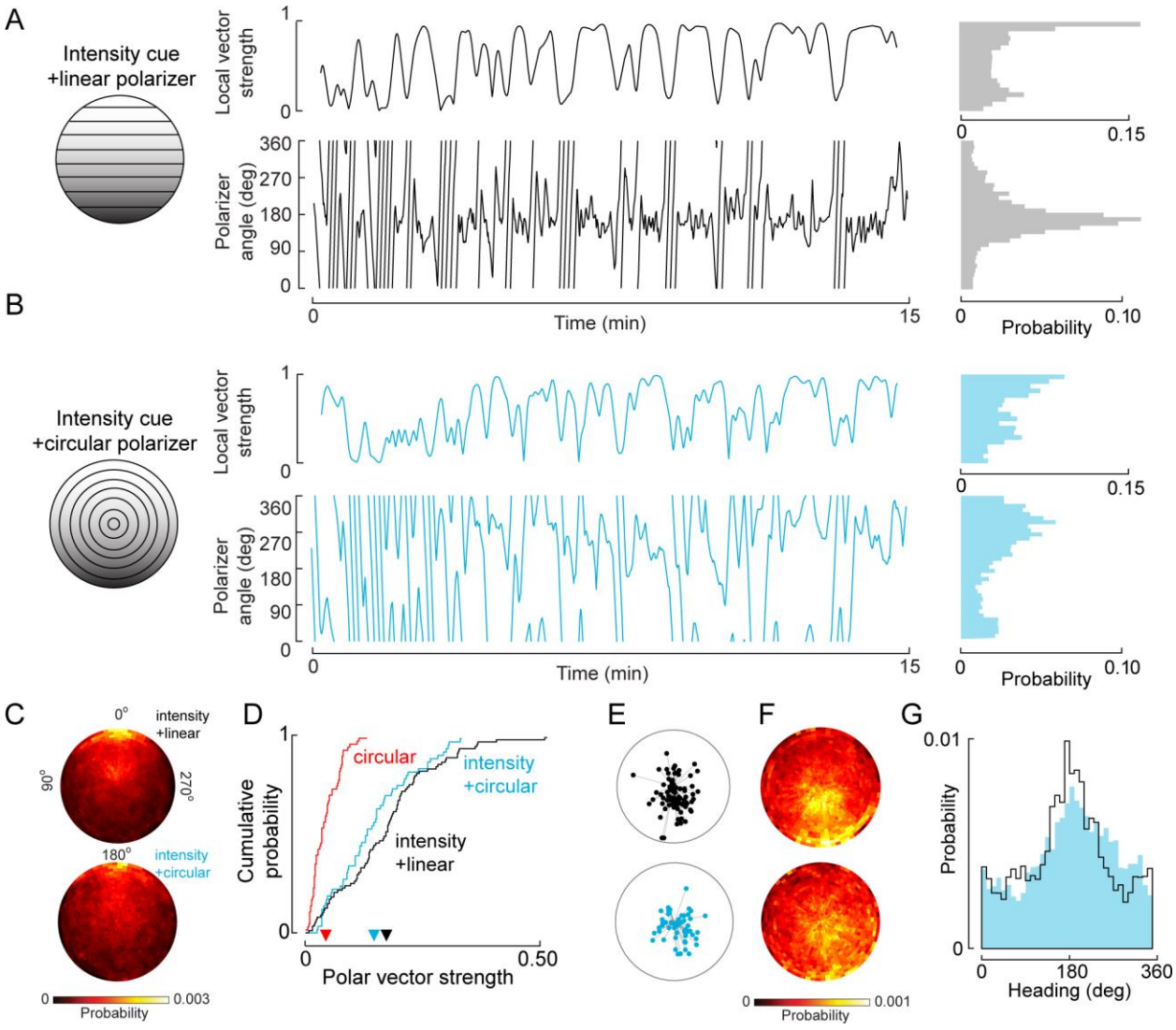

Figure 6. *Drosophila* can integrate polarized light with intensity cues to maintain a stable flight heading. (A) Example trial in which the linearly polarizing filter was superimposed with an intensity gradient; the plotting conventions are as in Fig. 1E (λ= 470 nm, mean polar heading = 167.5°). (B) Example trial in which the circularly polarizing filter was superimposed with an intensity gradient (mean polar heading = 280.6°). (C) Occupancy histogram for intensity + linear polarizer (top) and intensity+circular polarizer (bottom). Data are aligned to mean heading; plotting conventions as in Fig. 2C. (D) Cumulative histogram of polar vector strength values for intensity + circular polarizer (blue, N=59), intensity + linear polarizer (black, N=88), and circular polarizer with no intensity gradient (red, N=66). Distribution means are plotted as inverted triangles. (E) Mean headings plotted versus vector strength (radial distance from center) for intensity + linear polarizer

(top panel) and intensity + circular polarizer (bottom panel). (F) Occupancy histograms for intensity + linear polarizer (top) and intensity + circular polarizer (bottom); data are not aligned to mean heading. (G) Heading distributions for intensity stimuli with linear (black outline) and circular (solid blue) polarizer, calculated using data in which local vector strength >0.8.

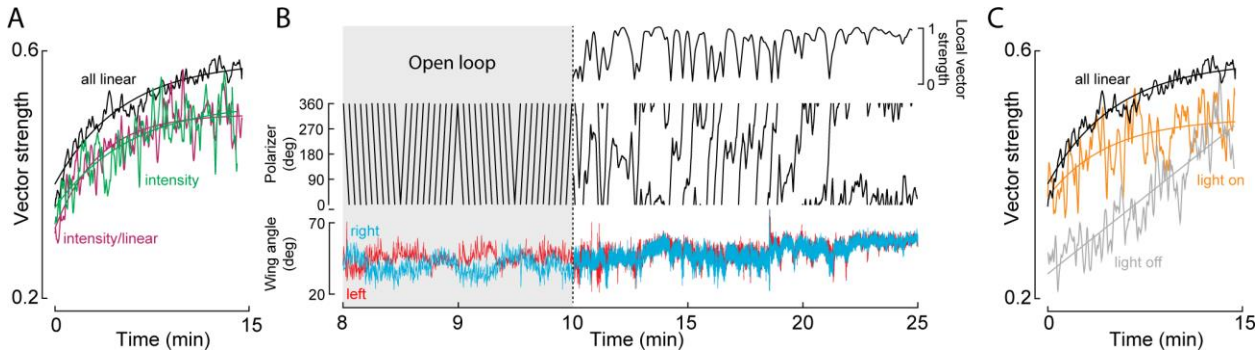

Figure 7. Local vector strength increases during flight under a variety of experimental conditions. (A) Local vector strength over 15-min flight for intensity+circular polarizer (green, N=59), intensity+linear polarizer (purple, N=88), and linear polarizer (black, N=372). Overlaid smooth lines are exponential fits. (B) Example experiment with open-loop exposure to polarized light prior to closed-loop flight. Note that the time scale changes at 10-min mark to illustrate open-loop stimulus. In addition, only the last two min of the open-loop epoch is shown. During the open-loop epoch, the polarizer rotated at 120° s^{-1}, switching direction every 30 sec. From 10-25 min, the polarizer angular velocity was coupled to wing stroke amplitude as in other closed-loop experiments. Local vector strength during the closed-loop epoch is plotted above. The bottom trace shows the wing stroke angles. (C) Rise in vector strength under three experimental conditions: 470 nm light on during 10-min open-loop epoch (orange, N=41), light off during open-loop epoch (grey, N=69), and data without pre-trial epoch (black, N=372).